Vol. 13(2), pp. 12-26, February 2019
DOI: 10.5897/AJPAC2018.0765
Article Number: AD20EC160230
ISSN: 1996 - 0840
Copyright ©2019
Author(s) retain the copyright of this article
http://www.academicjournals.org/AJPAC

African Journal of Pure and Applied Chemistry

Full Length Research Paper

Production and characterization of derived composite biosorbents from animal bone

Olafadehan O. A.*, Abhulimen K. E., Adeleke A. I., Njoku C. V. and Amoo K. O.

Department of Chemical and Petroleum Engineering, Faculty of Engineering, University of Lagos, Akoka-Yaba, Lagos 101017, Nigeria.

Received 27 July, 2018; Accepted 4 January 2019

Composite biosorbents were produced from animal bone by carbonization, activation of animal bone char with phosphoric acid and zinc (II) chloride independently, and the obtained activated carbons were separately impregnated on chitosan. The chitosan was produced from chitin, which was extracted from shrimp shell through deminerization, deproteinization and deacetylation processes. Comprehensive characterization studies were carried out on the chitin, chitosan, and the resulting five biosorbents via proximate and ultimate analyses, and Fourier-Transform Infrared (FTIR), Scanning Electron Microscope (SEM) and Electron-dispersive X-ray Spectroscopy (EDX) analyses. The absorption bands of the standard chitosan from Sigma-Aldrich and the experimentally prepared chitosan were in excellent agreement. The results of this study showed that activated carbons impregnated on chitosan have the potential to be applied as alternative efficient low-cost and eco-friendly biosorbents for batch and continuous adsorption column experimentation.

Key words: Biosorbents, chemical activation, chitin, chitosan, impregnation, characterization.

INTRODUCTION

The most imperative part in the adsorption process is the adsorbent. There is a variety of adsorbents (such as activated carbon, silica gel and alumina) that have been developed for a wide range of industrial applications because they present enormous surface areas per unit weight. However, the significance and relevance of activated carbon to an ever growing society cannot be overemphasized considering its wide applications in domestic, commercial and industrial settings (Mendez et al., 2006) in fluid phase adsorption studies. In the food industry, activated carbon is used in decolourization, deodorization and taste removal. It is used to remove heavy metals and organic contaminants from industrial wastewater. Activated carbon is used in water dechlorination and processing of foods. It is also used in medicine for adsorption of harmful chemicals and drugs. In gas cleaning applications, activated carbon is extensively used in air filters at industrial level as well as in general air conditioning application (Diets, 1990; Elliot et al., 1989; Inamullah et al., 2008; Oyo and Igbokwe, 2001). Owing to the fact that commercial activated carbon is very expensive and the processes of manufacturing and regeneration are not explicating enough (Bhattacharyya and Sharma, 2004), in recent

*Corresponding author. E-mail: oolafadehan@unilag.edu.ng. Tel: +234802 912 9559.

Author(s) agree that this article remain permanently open access under the terms of the Creative Commons Attribution License 4.0 International License

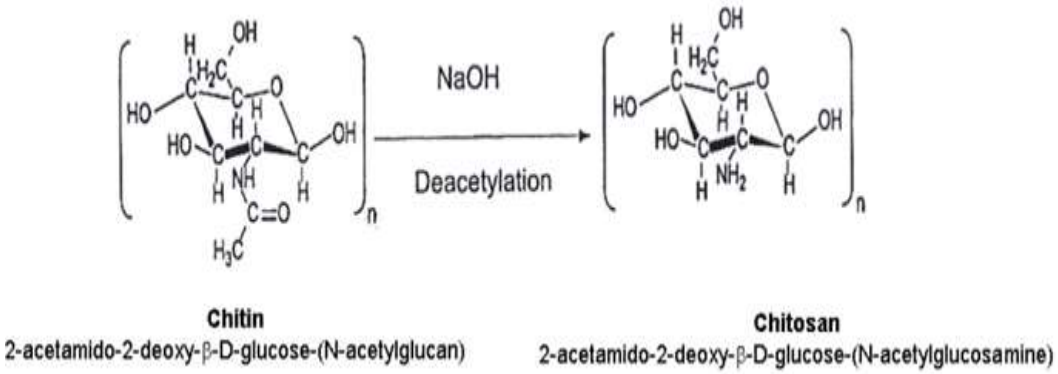

Figure 1. Chemical deacetylation of chitin to chitosan.

years, there is a growing interest in the use of low-cost and abundantly available lignocellulosic materials as precursors for the preparation of activated carbon. Amidst these materials, waste materials from agricultural by-products such as coconut shell, saw dust, bones of animals (cow and goats), and shells of crustaceans are economical and eco-friendly. This is due to their exceptional chemical composition, abundance, renewability, minimal cost, and efficiency in the treatment of industrial wastewater. However, the nature of the final product depends on the physical and chemical properties of the raw material used, the activation procedure (whether physical or chemical) and the process parameters during production (Guo and Lua, 2001; Leimkuehler, 2010). The surface modification of these activated carbons using surfactants may lead to difference in pore size distribution and surface polarity (Douglas et al., 1994), as well as proffering a better remediation for industrial purposes.

Every year, the industrial processing plants of fish and the fish markets do produce enormous crustaceans (shrimp, crab, prawns, lobster and krill) shells as fishery waste that pose environmental hazard. Shrimp shell was utilized in this study to develop added-value products which possess physicochemical and biological properties that find applications in many fields, including adsorption studies. Chitin, 2-acetamido-2-deoxy-β-D-glucose-(N-acetylglucan), is the second most abundant polymer in nature after cellulose. It occurs in nature as ordered crystalline micro fibrils forming structural components in the exoskeleton of anthropoids (Rinaudo, 2006), its major source is from exoskeleton of sea foods (crab, shrimp, prawn, and lobster shells), cartilage of the squid, and outer cover of insects, that are usually disposed as waste material. Depending on its source, three different crystalline polymorphic forms of chitin have been identified: α-chitin (shrimp and crab shells), β-chitin (squid pen), and γ-chitin (stomach cuticles of cephalopoda) (Jang et al., 2004). Chitosan, 2-acetamido-2-deoxy-β-D-glucose-(N-acetylglucosamine), is a biopolymer with free amine groups. It is produced on an industrial level by chemical deacetylation of chitin with a strong alkaline solution such as NaOH, as shown in Figure 1. Chitosan can also be produced by enzymatic deacetylation of chitin using lysozyme, snailase, neutral protease, and chitin deacetylase (Cai et al., 2006). Chitosan in itself has good adsorptive characteristics but it poses problems for developing commercial applications owing to its slight solubility at low pH, its active binding sites not readily available for sorption and its soft sites tendency to agglomerate or form gel in aqueous solutions. The transport of contaminants to the binding sites plays a very significant role in process design. Therefore, it is imperative to provide physical support and increase the accessibility of the metal binding sites for process applications (Okoya, 2016). However, impregnation of either char obtained from carbonaceous materials or of activated carbon on chitosan (Amuda et al., 2007; Ding et al., 2006; Nomanbhay and Palanisamy, 2005; Wu et al., 2002) has resulted in a diversity of adsorbents with far superior adsorption capacity.

The objective of this study is to contribute in the quest for low-cost and eco-friendly adsorbents that can be used for industrial applications via preparation of char from animal bone (referred to as animal bone carbon, ABC), chemical activation of the char using phosphoric acid and $ZnCl_2$, to produce acid-treated animal bone carbon (AABC) and $ZnCl_2$-treated animal bone carbon (ZABC) respectively, preparation of chitin from shrimp shell and subsequent preparation of chitosan from chitin, and impregnation of AABC and ZABC on chitosan to produce AABCC and ZABCC respectively, and then provide succinct information on the characterization properties of the five prepared adsorbents. The choice of adsorbents investigated in this study was motivated by the following rationale. Animal (cow) bone, an inexpensive naturally occurring material, is a component of animals. It is available in large quantities as a by-product from vertebrate animals. The shrimp shell from invertebrate crustaceans is a solid fishery waste being disposed thus

pave way for the preparation of the chitosan in this investigation for subsequent impregnation purposes.

MATERIALS AND METHODS

All the chemicals used were of analytical grade, purchased from Sigma Aldrich in Germany and used as received. These included phosphoric acid and zinc (II) chloride for chemical activation, NaOH (98%) and hydrochloric acid (HCl) (99%) for the preparation of chitosan as well as for pH adjustment, and oxalic acid dihydrate (99.9%) for the preparation of chitosan gel. Also, sodium chloride, iodine solution, sodium thiosulphate and potassium bromide were used at various stages of experimentation. Distilled deionized water was used throughout the experiments for preparing aqueous solutions.

Preparation of char from animal bone

Initially, the animal (cow) bone was thoroughly cleaned using tap water and soap to eradicate possible strange materials present in it (dirt, blood and sands etc). After this, distilled water was used to finally rinse it. The washed bone was sun-dried for 72 h. The carbonization process was carried out as previously described by Amuda and Ibrahim (2006) with a slight modification. The samples were placed in different large crucibles and the set up was kept in a muffle furnace at a temperature of 700°C for 3 h in the absence of air, after which they were removed and kept in a desiccator to allow them cool. Each sample was grounded to a size of 355 µm (44 BSS mesh size). 0.5 M HC1 was used to wash and purify the carbon. The product was rinsed several times with distilled water. The sample was then dried in an oven at 100°C for 2 h, and then stored. During this process, the volatile fraction and low molecular products of pyrolysis were removed. The equation for the carbonization process is shown in Equation 1:

$$\textbf{Animal bone} \xrightarrow{700^{0}C,\ 3h} \textbf{ABC + } \mathbf{CO_2} \quad (1)$$

Chemical activation of ABC using phosphoric acid and zinc (II) chloride

The chemical activation of the animal bone carbon (ABC) using phosphoric acid was carried out by the method previously described by Idowu (2015) with a slight modification. 450 g of ABC was charged into a crucible, mixed with 0.8 M of H_3PO_4 and was heated in the oven at 100°C for over 1 h till it formed a paste. The paste in a crucible was taken into a furnace where it was heated at 500°C for 3 h, allowed to cool to ambient temperature and was washed with de-ionized water several times until it reaches pH of 7 (checked by pH meter and litmus paper). It was dried in the oven at 100°C for 2 h. The final product was stored in air-tight polythene bag and put in a dessicator till further use. The equation for the activation process of ABC using phosphoric acid is represented in Equation 2:

$$\textbf{ABC} \xrightarrow{500^{0}C,\ H_3PO_4,\ 3h} \textbf{ABCC + } \mathbf{CO_2} \quad (2)$$

The chemical treatment of ABC using zinc (II) chloride was done according to Ningthoujam (2010) with slight modifications. 250 g of $ZnCl_2$ was added to 1000 ml of water and 250 g of animal bone char was gently added to the mixture and stirred. The mixture was allowed to stay for 24 h; it was drained and dried in the oven at 110°C for 3 h, washed with distilled water to remove traces of $ZnCl_2$ and dried in the oven 110°C for 1 h. The final product was stored in an air-tight polythene bag till further use. The equation for the activation process of ABC using zinc (II) chloride is shown in Equation 3:

$$\textbf{ABC} \xrightarrow{110^{0}C,\ ZnCl_2,1h} \textbf{ZABC + } \mathbf{CO_2} \quad (3)$$

Preparation of chitin from shrimp

The shrimp shell was washed with tap water, and then sun-dried for 4 days. It was later crushed using mortar and pestle into smaller particle sizes and sieved into 1 mm (18BSS). The sieved material was kept in a polyethylene bag at ambient temperature of 28±2°C for 24 h for partial autolysis to facilitate chemical extraction of chitin with a view to improving the quality of chitosan. Demineralization was performed by extracting chitin from shrimp shell as described by Toan (2009) with slight modification. 270 g of the sieved sample was weighed and put in a conical flask. 900 ml of 0.68 M of HCl solution was added (1:5w/v). The mixture was stirred using a griffin shaker at 28°C for 3 h. The resulting solution was filtered and washed till it reaches neutrality (blue litmus paper was used to check for the acidity). It was later scraped into petri dish and dried in the oven at 100°C for 3 h. After this process, deproteinization of the demineralized material was carried out by treating it with 600 ml of 0.60 M of NaOH to form a solution (1:3 w/v). The mixture was stirred and boiled in a water bath at 60°C for 4 h. The resulting solution was filtered and washed with distilled water to neutrality (red litmus paper was used to check if the base had been completely washed off). After washing, the mixture was filtered and the residue (chitin) scraped into a petri dish, and dried in the oven at 100°C for 3 h.

Preparation of chitosan

Deacetylation reaction was used to convert chitin to chitosan according to a revised procedure of Toan (2009). Then, a method described by Aderonke et al. (2014) was used for the preparation of chitosan gel (a whitish viscous gel). The degree of deacetylation of the chitosan was determined by applying the method used by Guibal et al. (1994). The molar mass of chitosan was determined by using the equation of Mark-Houwink-Sakurada for viscosity measurements at different concentrations.

Surface modification of AABC and ZABC with chitosan

The surface modification of AABC and ZABC with chitosan gel was carried out using the methods described by Aderonke et al. (2014) and Babel and Kurniawan (2004) respectively. 150 g of AABC was slowly added to 100 ml of chitosan gel diluted with 500 ml of water, and heated to 50°C and agitated at 150 rpm for 5 h. The resulting AABCC was then soaked in 0.5% NaOH solution till any residual acid was removed. The prepared AABCC was washed with deionized water and dried at 100°C for 2 h, cooled at room temperature and stored in desiccator for use. The same process was applied to 50 g of ZABC to obtain $ZnCl_2$-treated animal bone carbon impregnated on chitosan (ZABCC).

Characterization of different prepared adsorbents

Determination of surface area

The specific surface area of the activated carbon was estimated

Table 1. Proximate analysis of chitin and chitosan from shrimp shell.

Materials	Proximate analysis, %			
	Moisture content	Ash content	Protein	Fibre
Chitin	23.21	3.63	17.39	46.50
Chitosan	15.40	9.40	14.88	76.40

using Sear method (Alzaydian, 2009) by agitating 2 g of the different adsorbents prepared (ABC, AABC, AABCC, ZABC and ZABCC) separately in 100 ml of diluted hydrochloric acid at a pH of 3. Then, 30 g of NaOH was added while stirring the suspension and the volume was made up to 150 ml with deionized water. The resulting solution was titrated with 0.1 N NaOH to raise the pH from 4 to 9 and the volume, V_{OH}, of NaOH was recorded. The surface area, *S*, of each adsorbent was calculated using Equation 3:

$$S = 32V_{OH} - 25 \quad (3)$$

The remaining filtrate was cooled to room temperature and the pH was determined using pH meter.

Determination of ash content

The ash content (AC) of each adsorbent was determined by the method of Jeyakumar and Chandrasekaran (2014) by using Equation 4:

$$AC = \frac{M_1}{M \times (100 - X)/100} \times 100 \quad (4)$$

where *M* is the mass of sample taken for test, M_1 mass of ash, and *X* the % of moisture content present in sample taken for test.

Determination of bulk density

The apparent or bulk density, ρ_b, of each adsorbent was determined using the tapping procedure described by Ahmeda et al. (1997). 2 g of each sample of the adsorbent, after being dried at 105°C, was put into a 10 ml capacity graduated cylinder. The bottom of the cylinder was tapped gently on the laboratory bench top several times until there is no further reduction of the sample level. The bulk density was calculated according to the equation: $\rho_b = W/V_M$, where *W* is the weight of dry material, g; and V_M the volume of dry material, ml.

Determination of pH

The procedure of Jeyakumar and Chandrasekaran (2014) was used to obtain pH. 10 g of the dried sample was weighed and transferred into a 1 L breaker. 300 ml of freshly boiled water (adjusted to pH of 7.0) was added, and heated to boiling. After digesting for 10 min, the solution was then filtered while hot, rejecting the first 20 ml of the filtrate. The remaining filtrate was then cooled to room temperature and the pH was determined using a pH meter.

Determination of iodine number

The iodine number, *I*, was determined using the method previously described in ASTMD 4607-94 (2006), and is given by:

$$I = \frac{E \times V_B \times c \times 100}{w_s \times 1000} \quad (5)$$

where *E* is the equivalent weight of iodine (=127), V_B and *c* the volume and normality of sodium thiosulphate used respectively and w_s the weight of sample used in g.

Fourier-Transform Infrared (FTIR) analysis

The FTIR analyses of the adsorbents were determined using Shimadzu FTIR-8300 Spectrometer. The corresponding spectra of the chitosan and the derived composite biosorbents were obtained showing the wavelengths in the range 4000 to 400 cm^{-1} of the different functional groups in the samples which were identified by comparison with those in the library.

Scanning electron micrograph of adsorbents

The scanning electron micrograph (SEM) of each adsorbent was carried out using JEOL Scanning Electron Microscope whereby the surface texture and morphological characteristics of the adsorbents were clearly revealed.

RESULTS AND DISCUSSION

Characterization of chitin and chitosan from shrimp shell

Proximate analysis of chitin and chitosan

The proximate analyses of chitin and chitosan prepared from shrimp shell in this study are presented in Table 1. These analyses revealed that the chitin had higher moisture content than the chitosan, which was expected for reason of water being removed from the chitin prior to the chitosan production. The ash content of the chitin was far lower than that of the chitosan as a result of the presence of the acetyl group in the chitin sample. It should be noted that ash is the inorganic residue remaining after water and organic matter had been

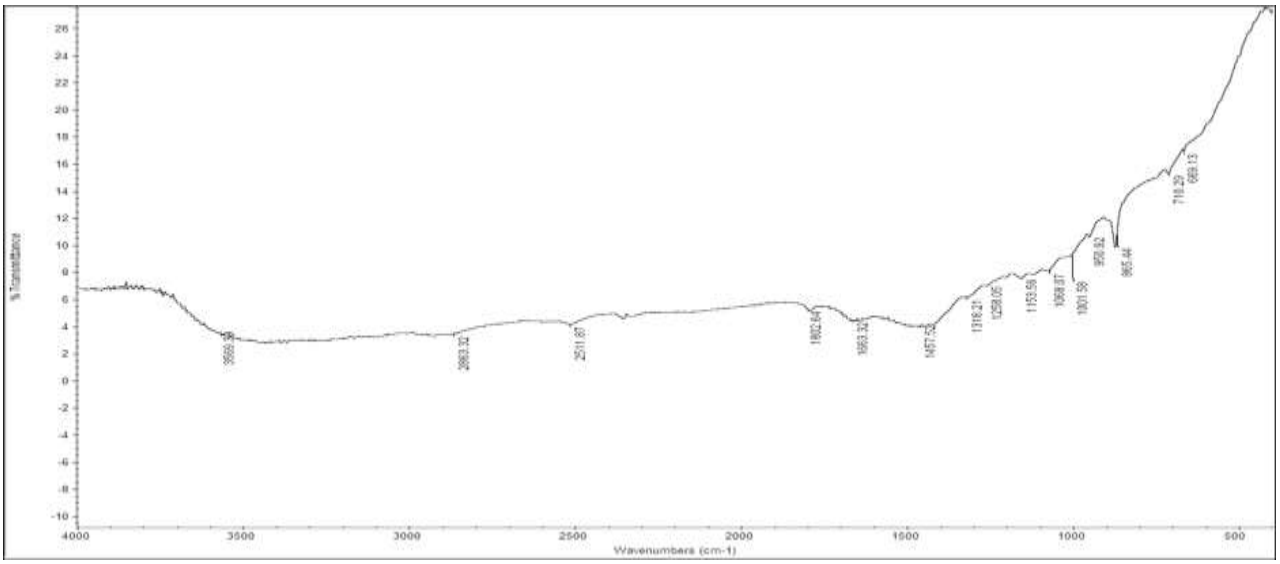

Figure 2. FTIR spectra of the chitin from shrimp shell.

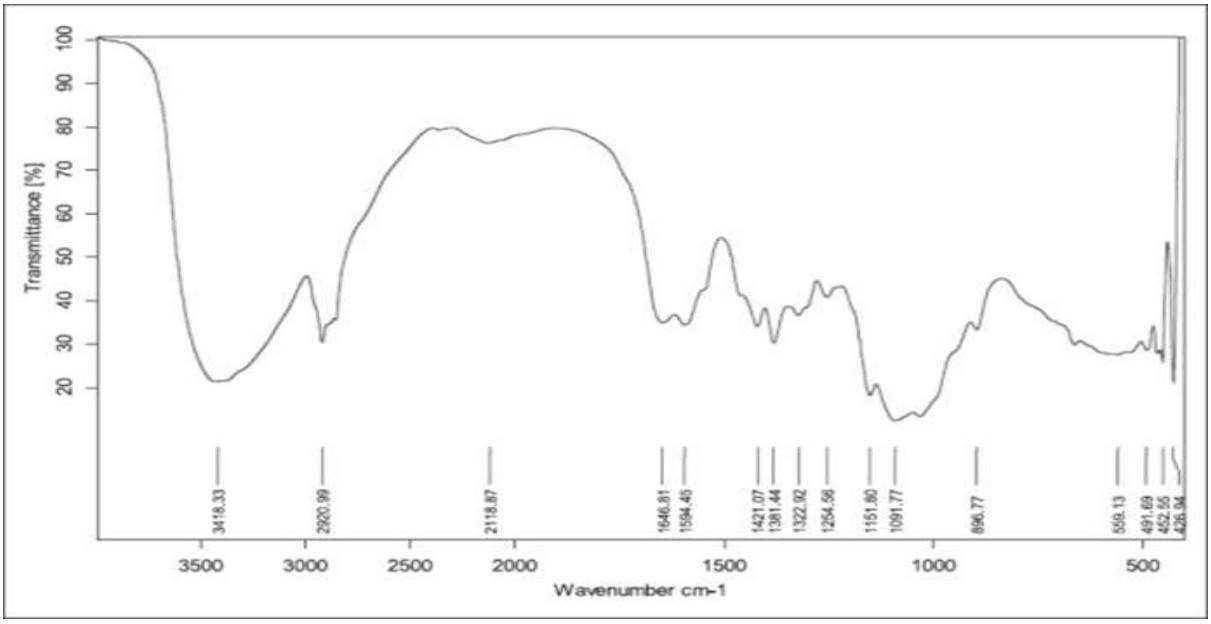

Figure 3. FTIR spectra of chitosan.

removed from a sample. Owing to the deproteinization of the chitin and its low degree of deacetylation of 4.02%, the protein content of the chitosan was less than that of the chitin. The fibre content of the chitosan was higher than that of the chitin owing to the fact that the removal of more matter from the chitin to obtain chitosan could have led to the presence of more fibre in the chitosan than in chitin.

The solubility of the chitosan was checked using four different solvents: water, ethanol, NaOH and concentrated ethanoic acid. It was found that the chitosan was soluble in acidic condition but insoluble in alkaline, ethanol and neutral solution. The pH value of the chitosan was found to be 10.35.

Fourier Transform Infrared (FTIR) characterization of chitin and chitosan from shrimp shell

Figures 2 and 3 show the FTIR spectra of chitin and

Table 2. Comparison of the characteristic absorption bands in the FTIR spectra of standard and experimentally prepared chitosan.

Wave number (cm^{-1})		
Chitosan from shrimp shell		Functional groups
Standard	Experimental	
3423	3418.33	NH_2 association in primary amines, OH association in pyranose ring
2923 –	2920.99 –	CH_2 in CH_2OH group
2121.8	2118.87	C=O in $NHCOCH_3$ group (amide I band)
1667	1648.81	Amide II band (N-H bending)
1597	1594.48	CH_2 in CH_2OH group
1422	1421.07	CH_3 in $NHCOCH_3$ group
1380	1381.44	Amide III band (C-N stretching)
1322	1322.92	Asymmetric bridge oxygen stretching (glycosidic linkage)
1155	1151.80	
1077	1091.77	C-O in secondary OH group
1031	1032	C-O in primary OH group
897	896.77	Pyranose ring stretching
664	663.80	N-H out of plane
616	616	O-H out of plane
Not provided	550.13	C-X group, where X is a halogen

chitosan respectively, where the % absorbance was plotted against wave number. Based on the FTIR spectra depicted for chitin, it was obvious that there was no prominent peak, compared with the one shown for chitosan. Figure 2 was shown to confirm the production of chitosan from chitin, wherein the peaks were assigned to various functional groups according to their respective wave numbers. Various absorption bands within the 4000-400 cm^{-1} range were recorded in the FTIR spectra of chitosan, prepared from shrimp shell. These bands were compared with those of standard chitosan from Sigma-Aldrich in Table 2. It was evident that there was excellent agreement between the absorption bands of standard chitosan and the experimentally prepared chitosan in this study.

The characteristic band at 3418.33 cm^{-1} could be assigned to the stretching vibrations of –NH, -OH, -NH_2 and intermolecular hydrogen bonds which overlap each other. The wave number at 2920.99 cm^{-1} suggested an aromatic ring functional group region. The observed peak at 2118.87 cm^{-1} was due to the presence of the methyl group in $NHCOCH_3$. The characteristic –NH band of chitosan indicated the presence of a carbonyl group at the observed band at 1648.81 cm^{-1} aromatic ring finger print region. It should be noted that the carbonyl group was due to the incomplete deacetylation of chitin to chitosan. The observed peak at 1594.48 cm^{-1} suggested Amide II band (N-H bending) (Argun and Dursun, 2006). The observed peak at 1421.07 cm^{-1} suggested aromatic ring finger print region. The wave numbers 1381.44 and 1322.92 cm^{-1} suggested aromatic rings in the finger print region. The observed band at 1151.80 cm^{-1} suggested asymmetric bridge oxygen stretching (glycosidic linkage). The observed peaks at 1091.77 and 1032 cm^{-1} suggested C-O in secondary and primary OH group respectively. The observed peak at 896.77 cm^{-1} suggested pyranose skeletal vibrations. The bands at 663.80 and 616 cm^{-1} were assigned to N-H and O-H out of plane respectively, while the observed band at 550.13 cm^{-1} was assigned to C-X group, where X is a halogen.

Determination of degree of deacetylation of chitosan

IR technique was used for the determination of the degree of deacetylation, *DD*, of chitosan, according to the methods described by Domszy and Roberts (1985) and Hiral et al. (1991) using Equation 6:

$$DD = 100\left(1 - \frac{A_{159445}}{A_{292099}} \times \frac{1}{1.33}\right) \quad (6)$$

where A_{159445} and A_{292099} are values of absorbance at the wavelengths 1594.45 and 2920.99 cm^{-1} respectively, and the factor 1.33 denotes the value of the ratio of A_{159445} to A_{292099} for fully N-acetylated chitosan. From the FTIR analysis of chitosan, the % transmittances at the wavelengths 1594.45 cm^{-1} and 2920.99 cm^{-1} were obtained, which was then converted to absorbance (=2-log (% transmittance)) to determine the degree of deacetylation of the prepared chitosan from shrimp shells as 95.98%, using Equation 6. This value was in the range (56-99%) given by No and Meyers (1995), No et al. (2000)

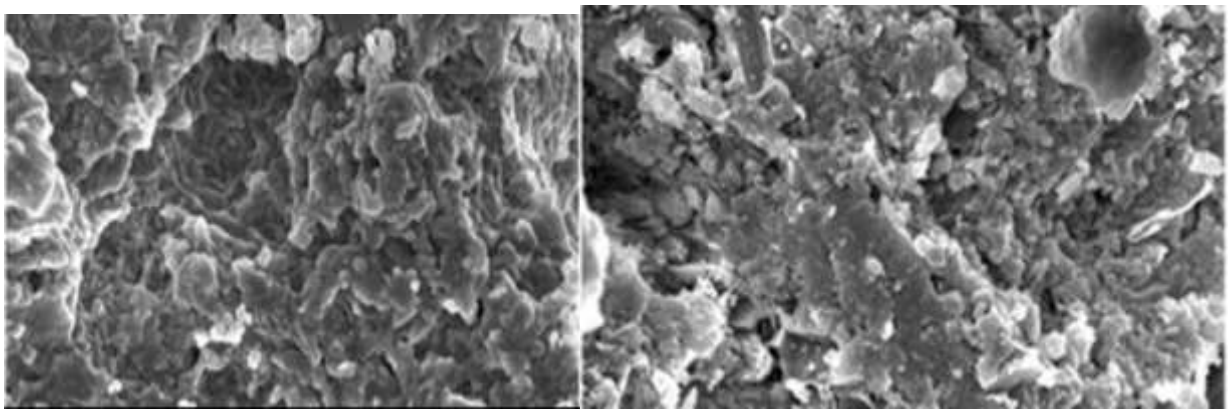

(a) (b)

Figure 4. SEM image of chitosan at (a) magnification of 10000; (b) at magnification of 12000.

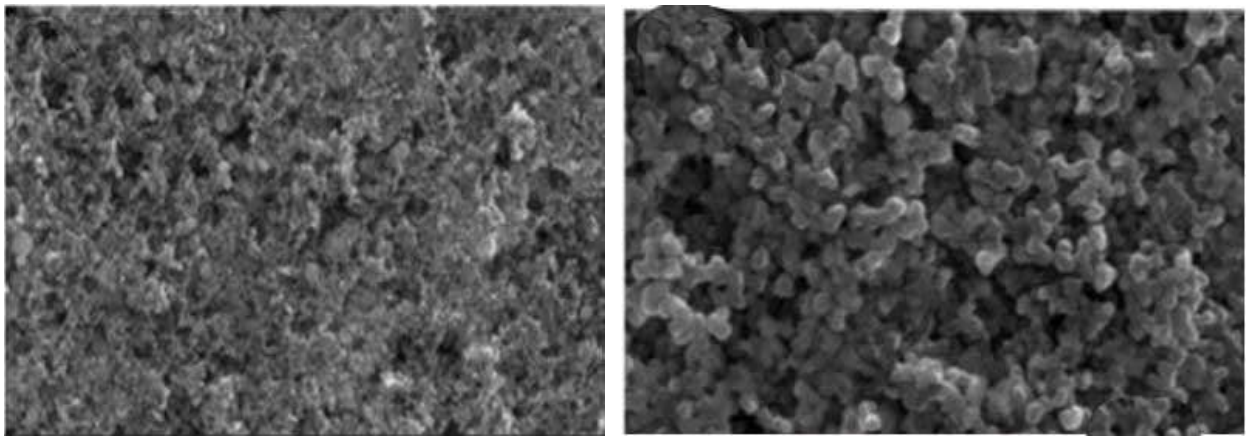

(a) (b)

Figure 5. SEM image of animal bone carbon at (a) magnification of 10000; (b) at magnification of 12000.

and Martino et al. (2005), with an average of 80%, depending on the crustacean species and the preparation methods.

Surface morphology of chitosan

JEOL Scanning Electron Microscope (SEM) (model: JSM 7600F) was used to observe the pore structure of the prepared chitosan and animal bone carbon. Figure 4a and b showed the scanning electron microscope images of chitosan produced from shrimp shells at 10000 and 12000 magnifications respectively. The SEM images of animal bone carbon produced from animal bone at 10000 and 12000 magnifications respectively were depicted in Figure 5a and b.

In Figures 4 and 5, the SEM photographs showed a clustered surface with wide varieties of pores present in the prepared chitosan and animal bone carbon, which were more visible at 12000 magnifications with respective average diameters of 5 µm and 2 µm for the chitosan and animal bone carbon. The Energy Dispersive X- ray spectroscopy (EDX) of the prepared chitosan revealed the presence of elements such as carbon (14.20%), silicon (12.30%), oxygen (10.72%), copper (32.10%), zinc (25.35%) and iron (6.55%) in the prepared chitosan, as shown in Figure 6. Similar results were obtained for the animal bone carbon and the derived composite biosorbents with differences in the percentage of elements present being less than ± 0.05 (Figures not shown). The presence of elements such as Zn, Cu, and Fe enhances adsorption of heavy metals through ion

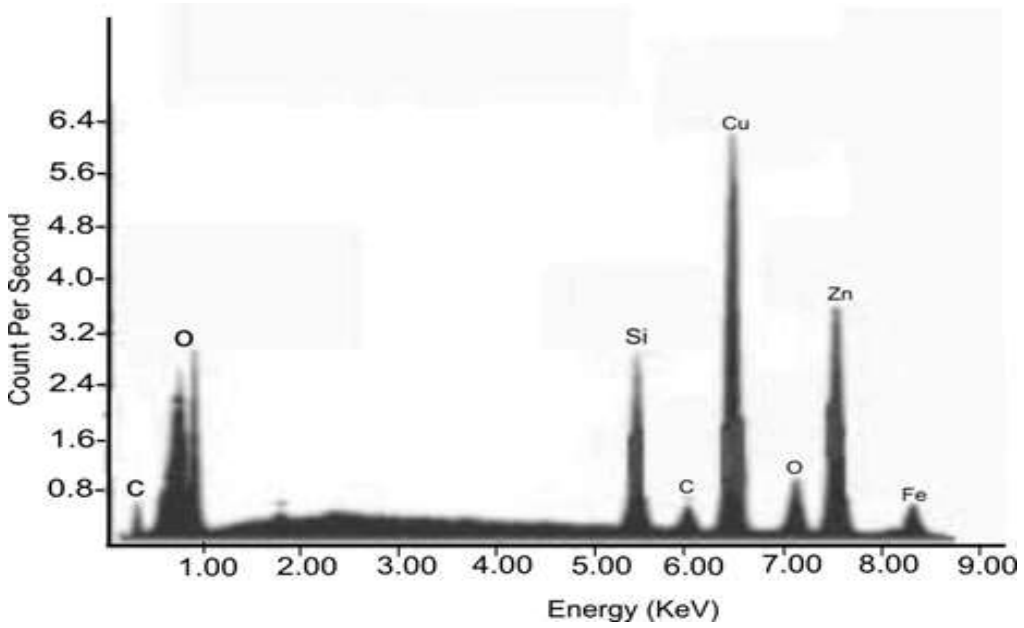

Figure 6. EDX spectra of chitosan.

Table 3. Ultimate and proximate analyses of animal bone.

Ultimate analysis (%)					Proximate analysis (%)			
C	**H**	**N**	**S**	**O**	**Moisture content**	**Ash content**	**Volatile matter**	**Fixed carbon**
49.70	1.72	0.20	0.10	48.30	5.50	0.40	75.40	1.50

exchange while elements such as O and Si prompt chelation, coordination and complexation reactions.

Ultimate and proximate analyses of animal bone

The results of the ultimate and proximate analyses of the animal bone are given in Table 3. From the ultimate analysis, the precursor for the preparation of different adsorbents investigated in this study had very low nitrogen and very low sulphur content and thus cannot contribute to environmental issues involving oxides of nitrogen and sulphur. Also, the animal bone has a high volatile matter content and low ash content, which is essential for pyrolysis and gasification processes.

The lignocellulosic composition of the animal bone was determined according to the Robertson and Van Soest (1981) method. Here, the analysis showed the presence of carbohydrate polymers (45.90% cellulose and 14.90% hemicellulose), and an aromatic polymer (39.20% lignin). These carbohydrate polymers contain different sugar monomers (six and five carbon sugars) and they are tightly bound to lignin. They influence the microstructural properties of the carbon. Lignin is the least reactive substance as compared to cellulose and hemicellulose, it contributes to the solid yield of the thermal process, which definitely influences the final porosity development. The lignin content of the animal bone investigated in this study was comparatively high and thus the precursor would be candidates for the production of a more micropore activated carbon. Heterogeneous pore size distribution depends on cellulose content. High hemicellulose content is associated with having a broader particular pore size distribution in relation to cellulose and lignin.

Characterization of the prepared adsorbents

The proximate analysis of a material is the most often used analysis for characterizing it in connection with its utilisation as an adsorbent. Table 4 presents the characteristics of the five adsorbents (ABC, AABC, AABCC, ZABC and ZABCC) prepared in this study.

Higher moisture content reduces the adsorption capacity of carbon by diluting the action of activated carbon. From Table 4, the moisture content of AABCC

Table 4. Proximate analysis and physicochemical properties of the prepared adsorbents.

Proximate analysis	Adsorbents				
	ABC	AABC	AABCC	ZABC	ZABCC
Moisture content (%)	22.50	17.65	14.40	21.20	18.70
Ash content (%)	6.65	6.00	2.14	8.24	8.12
Volatile matter (%)	7.76	7.76	7.54	7.74	7.60
Fixed carbon (%)	62.42	12.20	10.71	13.10	11.50
Physicochemical properties					
Surface area (m^2/g)	300	397.40	413.40	343	370.20
Bulk density (g/ml)	1.008	1.088	1.687	1.1907	1.4712
pH	8.0	8.33	8.57	8.10	8.62
Iodine value (mg/g)	310	360	470	330	430

was 14.40%, which was the least amongst the five carbons prepared, followed by AABC. Hence, the increasing order of the proposed utilisation of these five carbons as adsorbent is ABC<ZABC<AZBCC< AABC<AABCC, implying that AABCC could be adjudged the best adsorbent in this study. During carbonization, ash content is the inorganic, inert, amorphous and unstable portion present in the activated carbon and it arises from basic nature of raw material (Jeyakumar and Chandrasekaran, 2014). Table 4 reveals that the ash content of AABCC was 2.14% which is the least amongst the five prepared carbon. The lower the ash content, the better the starting material for use as adsorbent. Hence, this investigation revealed that AABCC would be a better adsorbent than the other four adsorbents. The obtained value for AABCC was favourable because the ash content serves as interference during the adsorption process (Khan et al., 2009). AABCC has a lower volatile matter than ABC, AABC, ZABC and ZABCC. This could be attributed to the fact that during thermal activation, most of the non-carbon elements such as hydrogen, oxygen, nitrogen and sulphur might have been eliminated as volatile gaseous products by the carbonization process. There is a little difference in terms of fixed carbon content of AABC, AABCC, ZABC and ZABCC, implying that these carbons are viable options for use as adsorbents in adsorption studies.

The surface area of an activated carbon is directly related to its porosity, and in part to its activity as an adsorbent. From Table 4, the increasing order of surface areas of the prepared adsorbents is ABC<ZABC< ZABCC<AABC<AABCC. Hence, AABCC could be adjudged the best and highly porous adsorbent in this study. However, the surface areas of these adsorbents conformed to the range for plant adsorbents, which is between 10^2 and 10^3 m^2/g. The experimental results of bulk density of the prepared adsorbents revealed that AABCC had the highest bulk density, which is indicative of higher quality adsorbent than the other four adsorbents. Thus, AABCC would thus provide greater volume activity thereby resulting in better contact with the adsorbate, leading to effective adsorption process. The pH parameter is a factor affecting adsorption capacity of adsorbate. It is well known that pH could affect the protonation of functional group on plantain peel as well as metal chemistry (Tsezos and Bell, 1989). The pH values of ABC, AABC, AABCC, ZABC and ZABCC were determined to be 8.0, 8.33, 8.57, 8.10 and 8.62 respectively, as shown in Table 4. These values were in agreement with the findings of Cheremisnoff and Ellerbusch (1978) that the pH of either raw or carbonized materials in water suspension can vary between 4 and 12. Iodine value is a fundamental parameter used to characterize the performance of activated carbon. It is a measure of the micropore content of the activated carbon and is obtained by the adsorption of iodine from solution by the activated carbon sample (Jeyakumar and Chandrasekaran, 2014). Higher value of the iodine value indicates higher degree of activation. The iodine values of ABC, AABC, AABCC, ZABC and ZABCC are given in Table 4. The AABCC had the highest iodine value of 440 mg/g, indicating that its pore surface and structure were the best developed in this study. However, the iodine numbers obtained in this study for the different five carbons are in the range for commercial adsorbents: 300 to 1200 mg/g (Jeyakumar and Chandrasekaran, 2014).

Fourier Transform Infrared (FTIR) characterization of prepared adsorbents

Figure 7 depicts the FTIR spectra of animal bone carbon, where the various functional groups present in ABC were revealed in the 4000 to 500 cm^{-1} wavelength, as presented in Table 5. The broad band positioned at 3559.89 cm^{-1} revealed the existence of –OH stretching of the hydroxyl group. The 2359.89-2204.75 and 2014.78 cm^{-1} bands showed the presence of an alkyne group, C≡C. The peaks at 1416.36 cm^{-1} indicated C=C groups present in carbon. The observed bands at 1099.74 and1039.58 cm^{-1} indicated the presence of a phosphate group, or CO stretching of alcohol group or carboxylic

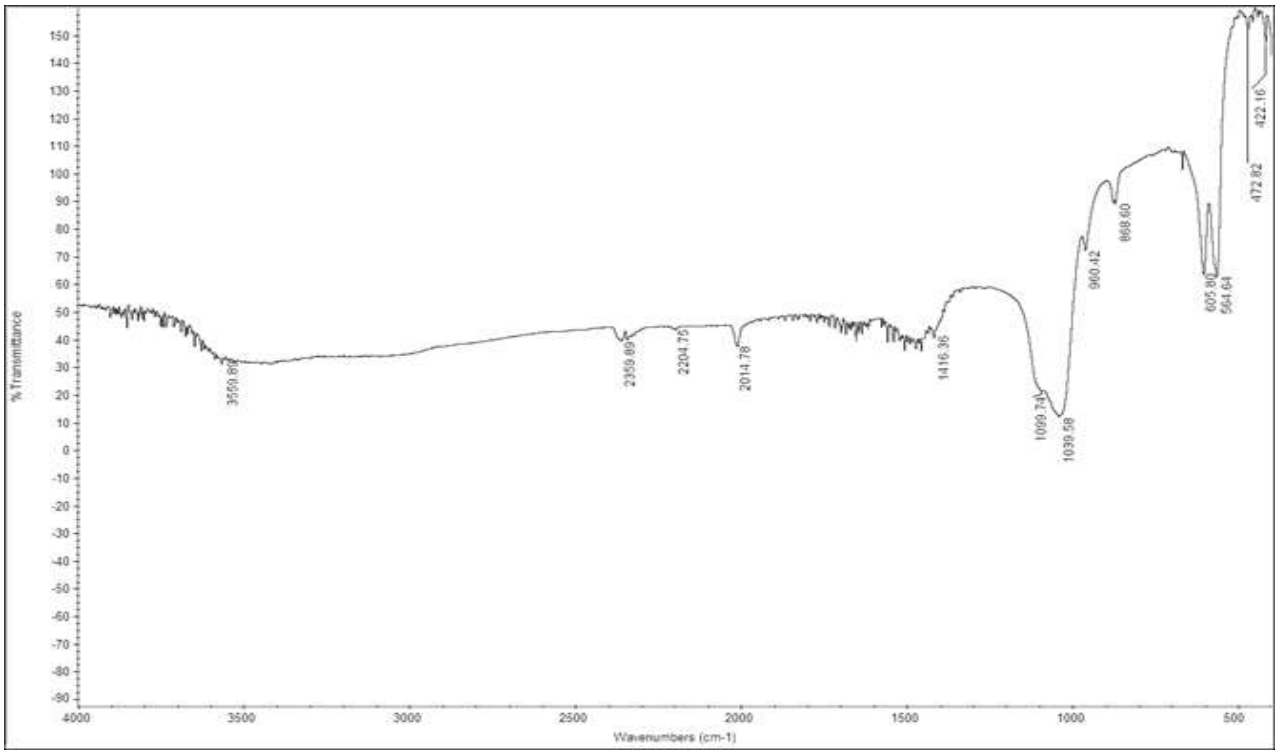

Figure 7. FTIR spectra of animal bone carbon (ABC).

Table 5. Characteristic absorption bands in the FTIR spectra of animal bone carbon.

Wavelength (cm^{-1})	Functional group
3559.89	-OH stretching of the hydroxyl group
2359.89-2014.78	C≡C
1416.36	C=C, O-H
1099.74-1039.58	PO_4^{3-} , CO stretching for alcohol or carboxylic acid
960.42-868.60	C=H bending of aromatics
605.80-564.64	C-X, where X is a halogen

acid. The peaks around 960.42-868.60 cm^{-1} showed the appearance of C=H group present in surface of carbon. The peaks between 605.80-564.64 cm^{-1} indicated the presence of C-X group, where X is a halogen.

Figure 8 shows the FTIR spectra of acid-treated animal bone carbon (AABC) while the different bonds present in it from the FTIR analysis are presented in Table 6. The broad band positioned at 3027.97 cm^{-1} indicated the presence of O-H bond. The bands between 2917.15 and 2207.92 cm^{-1} showed the presence of C-H stretching while the band at 2011.61 cm^{-1} indicated the presence of an alkyne functional group (-C≡C-). The band at 1419.53 cm^{-1} showed C-F stretching. However, between 1090.24 and 1036.41 cm^{-1} wavelengths, the band width revealed the existence of C=O stretching. At band width of 871.77 cm^{-1}, C=H bending of aromatics was attributed. The observed band at 602.64 cm^{-1} was as a result of the stretching of halogenated compounds where 'X' represent halogens (chiefly chlorine).

Figure 9 shows the FTIR spectra of acid-treated animal bone carbon impregnated on chitosan (AABCC), where the various functional groups present in it were revealed in the 4000 to 500 cm^{-1} wavelength, as presented in Table 7.

The broad band positioned at 3059.63 cm^{-1} revealed the existence of –OH stretching of the hydroxyl group. The 2014.78 cm^{-1} band showed the presence of an alkyne group, (C≡C). The peaks around 1612.66 cm^{-1} corresponded to the C=O stretching that might be attributed to the lignin aromatic groups. The peak at 1467.02 cm^{-1} indicated C=C groups present in carbon. The observed bands at 1406.86 and 1311.87 cm^{-1}

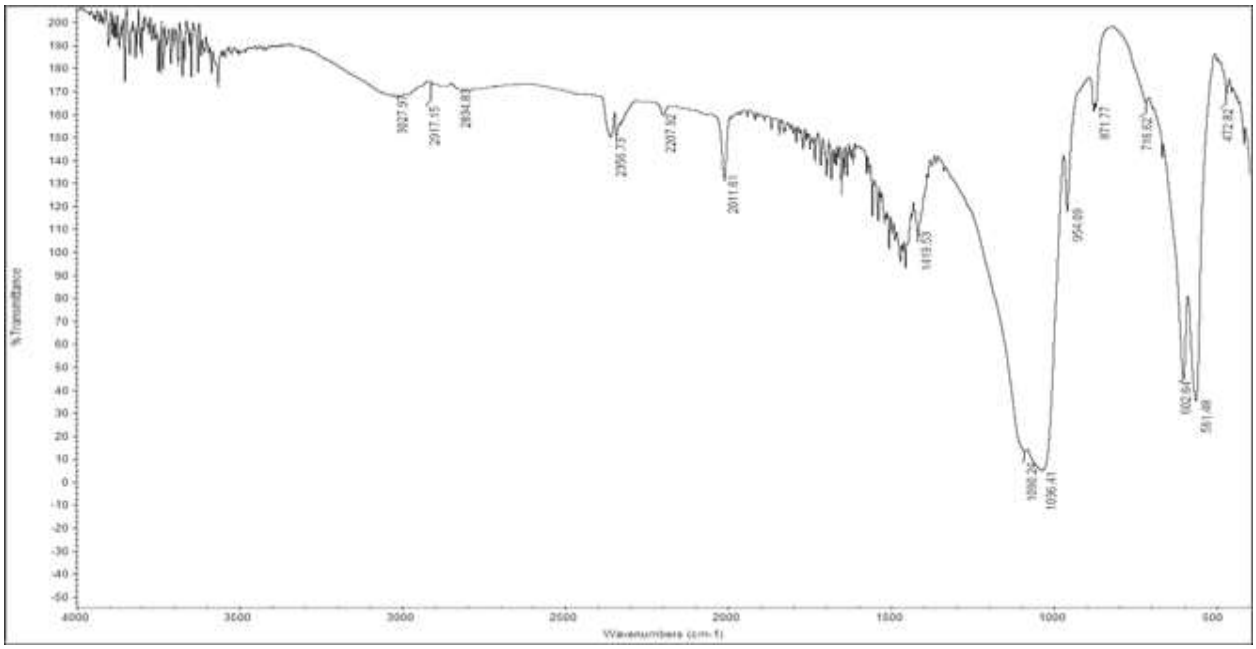

Figure 8. FTIR spectra of acid-treated animal bone carbon (AABC).

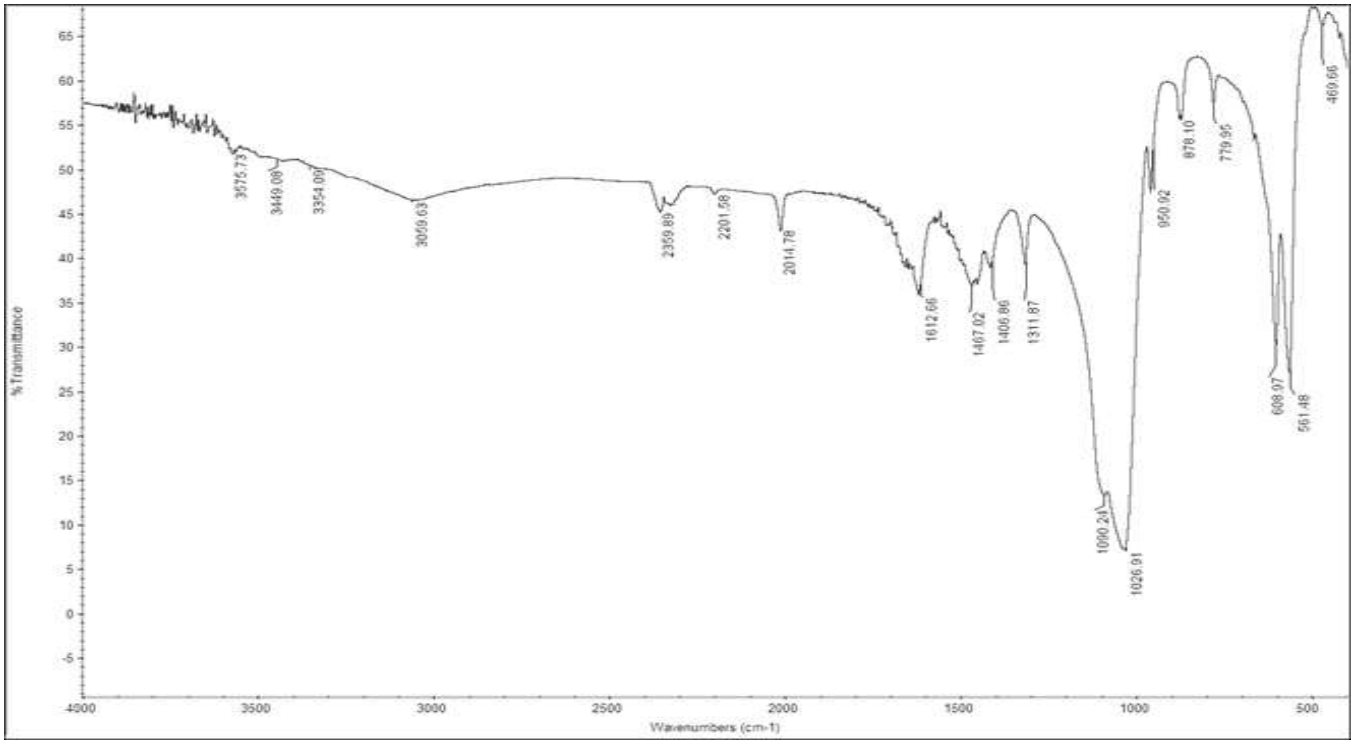

Figure 9. FTIR spectra of acid-treated animal bone carbon impregnated on chitosan (AABCC).

indicated C-F stretching while bands at 1090.24 and 1026.91 cm^{-1} indicated the presence of a phosphate group, or CO stretching of alcohol group or carboxylic acid. The peaks around 878.1 cm^{-1} showed the appearance of C=H stretching of aromatics. The peaks at 608.97 cm^{-1} indicated the presence of C-X group,

Table 6. Characteristic absorption bands in the FTIR spectra of acid-treated animal bone carbon (AABC).

Wavelength (cm^{-1})	Functional group
3027.97	-OH stretching of the hydroxyl group
2917.15-2207.92	C-H stretching
2011.61	C≡C
1419.53	C-F stretching
1090.24-1036.41	C=O stretching
871.77	C=H bending of aromatics
602.64	C-X, where X is a halogen

Table 7. Characteristic absorption bands in the FTIR spectra of acid-treated animal bone carbon impregnated on chitosan (AABCC).

Wavelength (cm^{-1})	Functional group
3059.63	-OH stretching of the hydroxyl group
2014.78	C≡C stretching
1612.66	C=O stretching
1467.02	C=C stretching
1406.86-1311.87	C-F stretching
1090.24-1026.91	PO_4^{3-}, C-O stretching for alcohol or carboxylic acid
878.10	C=H bending of aromatics
608.97	C-X, where X is a halogen

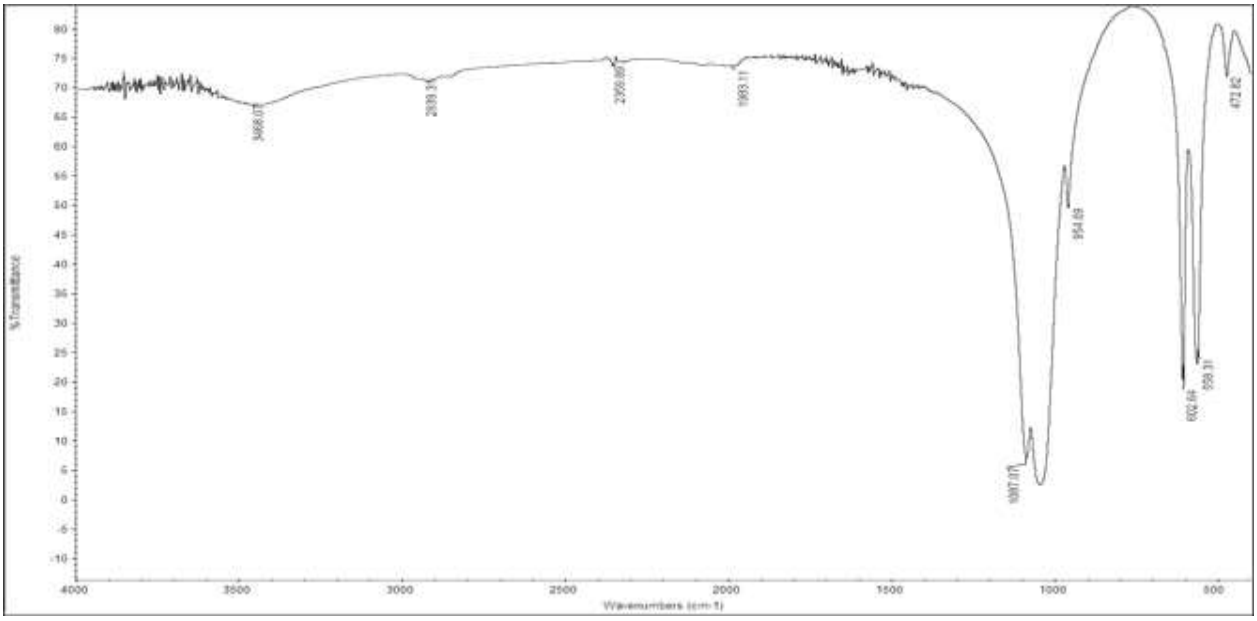

Figure 10. FTIR spectra of zinc (II) chloride-treated animal bone carbon (ZABC).

where X is a halogen. Figure 10 shows the FTIR spectra of $ZnCl_2$-treated animal bone carbon (ZABC) while the different bonds present in it from the FTIR analysis are presented in Table 8.

The 3468.07 cm^{-1} band showed the presence of O-H stretching of hydroxyl group. The 2939.31- 2359.89 cm^{-1} band showed the presence of an alkyne group, (C≡C). The bands at 1983.11 cm^{-1} corresponded to C=O

Table 8. Characteristic absorption bands in the FTIR spectra of zinc (II) chloride-treated animal bone carbon (ZABC).

Wavelength (cm^{-1})	Functional group
3468.07	-OH stretching of the hydroxyl group
2939.31-2359.89	C≡C
1983.11	C=O stretching
1087.07	PO_4^{3-}, CO stretch for alcohol or carboxylic acid
954.09	C=H bending of aromatics
602.64-558.31	C-X, where X is a halogen

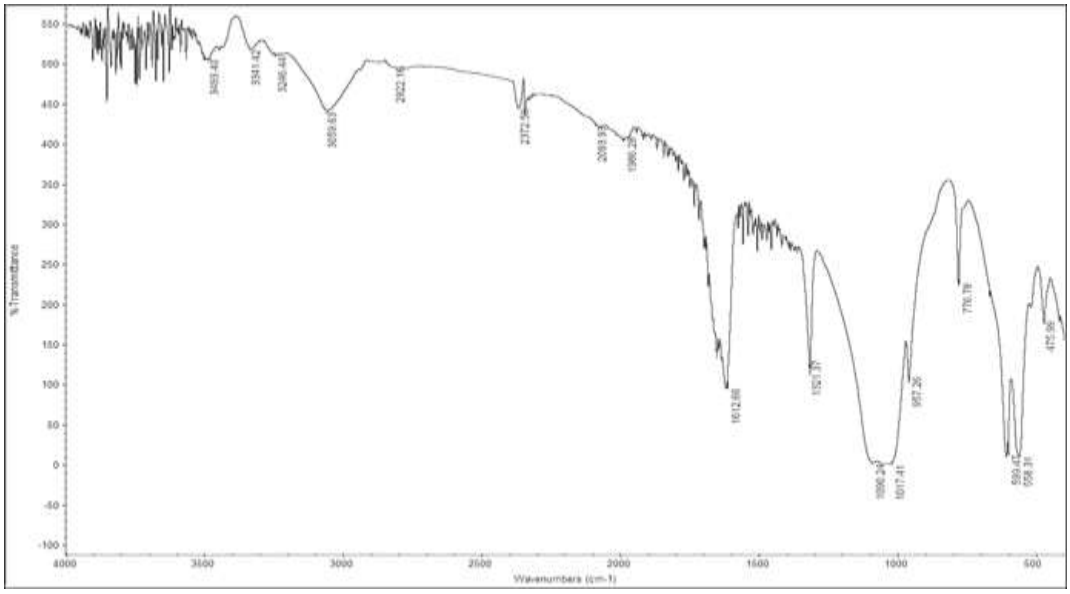

Figure 11. FTIR spectra of zinc (II) chloride-treated animal bone carbon impregnated on chitosan (ZABCC).

Table 9. Characteristic absorption bands in the FTIR spectra of zinc (II) chloride-treated animal bone carbon impregnated on chitosan (ZABCC).

Wavelength (cm^{-1})	Functional group
3493.40-3059.63	-OH stretching of the hydroxyl group
2822.16-2093.93	C≡C stretching
1986.28-1612.66	C=O, O-H stretching
1321.27	C=C stretching
1090.24-1017.41	PO_4^{3-}, C-O stretching for alcohol or carboxylic acid
957.26-776.78	C=H bending of aromatics
599.47-558.31	C-X, where X is a halogen

stretching that might be attributed to the lignin aromatic groups. The observed band 1087.07 cm^{-1} indicated the presence of a phosphate group, or CO stretching of alcohols and carboxylic acid. The peaks around 954.09 cm^{-1} showed the appearance of C=H group present in surface of carbon. The peaks between 602.64-558.31 cm^{-1} indicated the presence of C-X group, where X is a halogen.

Figure 11 shows the FTIR spectra of zinc (II) chloride-treated animal bone carbon impregnated on chitosan (ZABCC), where the various functional groups present in it were revealed in the 4000-500 cm^{-1} wavelength, as presented in Table 9. The broad band positioned at 3493.40-3059.63 cm^{-1} revealed the existence of –OH

stretching of the hydroxyl group. The 2822.16-2093.93 cm^{-1} band showed the presence of an alkyne group, (C≡C). The peaks around 1986.28-1612.66 cm^{-1} corresponds to the C=O and O-H stretching that may be attributed to the lignin aromatic groups. The peaks at 1321.37 cm^{-1} indicated C=C groups present in carbon. The observed band at 1090.24-1017.41 cm^{-1} indicated the presence of a phosphate group, or CO stretching of alcohol group or carboxylic acid. The peaks around 957.26-776.78 cm^{-1} showed the appearance of C=H group present in surface of carbon. The peaks between 599.47 and 558.31 cm^{-1} indicated the presence of C-X group, where X is a halogen.

Conclusion

Animal (cow) bone carbon was carbonized to produce animal bone carbon, which was subsequently activated with phosphoric acid and $ZnCl_2$ independently to produce AABC and ZABC. The prepared activated adsorbents were impregnated on chitosan to obtain AABCC and ZABCC. The results showed that activation of ABC improved its surface area and impregnation of AABC and ZABC on chitosan derived from shrimp shell enhanced further their respective specific surface areas. Comprehensive characterization studies were carried out on the chitin, chitosan, and the resulting five biosorbents via proximate and ultimate analyses, and FTIR, SEM and EDX analyses. The results of this study revealed that the use of animal bone and shrimp shells to produce activated carbons and composite adsorbents potentially provides less costly and eco-friendly adsorbents, processed from renewable resources.

CONFLICT OF INTERESTS

The authors have not declared any conflict of interests.

REFERENCES

Aderonke AO, Abimbola BA, Ifeanyi EO, Amuda OS, Oluwagbemiga SA, Oladotun WM (2014). Adsorption of heavy metals ions onto chitosan grafted coca husk char. African Journal of Pure and Applied Chemistry 8(10):147-161.

Ahmeda M, Marshall WE, Rao RM (1997). Potential of agricultural by product based activated carbon for use in raw sugar decolourisation. Journal of Science of Food and Agriculture 75:117-124.

American Society for Testing and Materials (ASTM) (2006). Standard test method for determination of Iodine number for activated carbon. ASTM Philadelphia P A. 4607-94.

Amuda OS, Giwa AA, Bello IA (2007). Removal of heavy metal from industrial wastewater using modified activated coconut shell carbon. Biochemical Engineering Journal 36(2):174-181.

Amuda OS, Ibrahim AO (2006). Industrial wastewater treatment for chemical oxygen demand (COD) using natural material as adsorbent. African Journal of Biotechnology 5(16):1483-1487.

Argun ME, Dursun S (2006). Removal of heavy metal ions using chemically modified adsorbents. Journal of International Environmental Application and Science 1:27-38.

Babel S, Kurniawan TA (2004). Cr(VI) removal from synthetic wastewater using coconut shell charcoal and commercial activated carbon modified with oxidizing agent and/or chitosan. Chemosphere 54(7):951-967.

Bhattacharyya KG, Sharma A (2004). Adsorption of Pb (II) from aqueous solution by Azadirachta indica (Neem) leaf powder. Journal of Hazardous Materials 113(1-3):97-109.

Cai J, Yang J, Du Y, Fan L, Qiu Y, Li J, Kennedy JF (2006). Enzymatic preparation of chitosan from the waste *Aspergillus Níger* mycelium of citric acid production plant. Carbohydrate Polymers 64:151-157.

Cheremisnoff P, Ellerbusch F (1978). Carbon Adsorption Handbook. Ann Anbor Science Handbook Publishing Incorporated 72:689-706.

Diets VR (1990). Bibliography of solid adsorption and United States cane sugar refineries and bone char manufactures. National Bureau Standards. Washington DC.

Ding P, Huang K, Li G, Liu Y, Zeng W (2006). Kinetics of adsorption of Zn (II) ion on chitosan derivatives. International Journal of Biology Macromolecules 39:222-227.

Domszy JG, Roberts GAF (1985). Evaluation of infrared spectroscopic techniques for analysing chitosan. Macromolecular Chemistry and Physics 186:1671-1682.

Douglas M, Farooq S, Knaebel K (1994). Pressure Swing Adsorption, New York, USA.

Elliot CG, Colby TV, Kelly TM, Hicks HG (1989). Charcoal lung: bronchiolitis obliterans after aspiration of activated charcoal. Chest 96(3):672-674.

Guibal E, Saucedo I, Jansson-Charrier M, Delanghe B, Le Cloirec P (1994). Uranium and vanadium sorption by chitosan and derivatives. Water Science and Technology 30:183-192.

Guo J, Lua AC (2001). Characterization of adsorbents prepared from oil palm shell by thermal activation for removal of gaseous pollutants. Material Science 55:334-339.

Hiral A, Odani H, Nakajima A (1991). Determination of degree of deacetylation of chitosan by 1H NMR spectroscopy. Polymer Bulletin 26:87-93.

Idowu EA (2015). Adsorption of selected heavy metals on activated carbon prepared from plantain (*Musa paradisiaca*) peel. M.Sc. Thesis, Department of Chemistry, Ahmadu Bello University, Zaria, Nigeria.

Inamullah B, Khadija Q, Kazi RA, Abdul KA (2008). Preparation and characterisation of chemically activated almond shells by optimization of adsorption parameters for removal of chromium (VI) from aqueous solutions. World Academy of Science, Engineering and Technology 34: 199-204.

Jang M, Kong B, Jeong Y, Hyung Lee C, Nah J (2004). Physicochemical characterization of α-chitin, β-chitin, and γ-chitin separated from natural resources. Journal of Polymer Science Part A: Polymer Chemistry 42:3423-3432.

Jeyakumar RP, Chandrasekaran V (2014). Adsorption of lead (II) ions by activated carbons prepared from marine green algae: Equilibrium and kinetics studies. International Journal of Industrial Chemistry 5 (2), doi:10.1186/2228-5547-5-2.

Khan A, Muthukrishnan M, Guha B (2009). Sorption and transport modelling of hexavalent chromium on soil media, Journal of Hazardous Materials 174:444-453.

Leimkuehler EP (2010). Production, Characterization, and Applications of Activated carbon, M. Sc. Thesis, University of Missouri, Missouri.

Martino AD, Sittinger M, Risbud MV (2005). Chitosan: A versatile biopolymer for orthopaedic tissue engineering. Biomaterials 5983-6002.

Mendez MOA, Lisboa ACL, Coutinhoand AR, Otani C (2006). Activated petroleum coke for natural gas storage. Journal of the Brazilian Chemical Society 17(6):1144-1150.

Ningthoujam S (2010). How to make activated charcoal, http://www.buzzle.com/articles/how-to-make-activated-charcoal.html

No HK, Lee KS, Meyers SP (2000). Correlation between physicochemical characteristics and binding capacities of chitosan products. Journal of Food Science 65(7):1134-1137.

No HK, Meyers SP (1995). Preparation and Characterization of Chitin and Chitosan-A Review. Journal of Aquatic Food Product Technology 4(2):27-52.

Nomanbhay SM, Palanisamy K (2005). Removal of heavy metal from

industrial wastewater using chitosan coated oil palm shell charcoal. Electronic Journal of Biotechnology 8(1):43-53.
Okoya AA, Akinyele AB, Ofoezie OS (2016). Chitosan-grafted carbon for the sequestration of heavy metals in aqueous solution. American Chemical Science Journal 11(3):1-14.
Oyo KB, Igbokwe PK (2001). Production of activated carbon from coconut-shell. Journal of Chemical Society of Nigeria 26(1):91-94.
Rinaudo M (2006). Chitin and chitosan: Properties and applications. Progress in Polymer Science 3:603-632.
Robertson JB, Van Soest PJ (1981). The Analysis of Dietary Fibre in Food, Marcel Dekker, New York.
Toan NV (2009). Production of chitin and chitosan from partially autolyzed shrimp shell. The Open Biomaterials Journal 1:21-24.
Tsezos M, Bell JP (1989). Comparison of the biosorption and desorption of hazardous organic pollutants by live and dead biomass. Water Resources 23:561-568.
Wu FC, Tseng RL, Juang RS (2002). Adsorption of dyes and humic acid from water using chitosan encapsulated activated carbon. Journal of Chemical Technology and Biotechnology 77:1260-1269.